Evidence of high Sr/Ca in a Middle Jurassic murolith coccolith species

Baptiste Suchéras-Marx[1] *, Fabienne Giraud[2, 3], Alexandre Simionovici[2, 3] **, Rémi Tucoulou[4], Isabelle Daniel[5]

[1] Aix Marseille Univ, CNRS, IRD, Coll France, CEREGE UM34, Aix-en-Provence, France

[2] Université Grenoble Alpes, ISTerre, Grenoble, France

[3] CNRS, ISTerre, Grenoble, France

[4] ESRF – The European Synchrotron Radiation Facility, Grenoble Cedex 9, France

[5] UMR CNRS 5276 LGL, Université Claude Bernard Lyon 1, Ecole Normale Supérieure Lyon, Villeurbanne Cedex, France

* Corresponding author: sucheras-marx@cerege.fr

**Institut Universitaire de France (IUF)

Abstract

Paleoceanographical reconstructions are often based on microfossil geochemical analyses. Coccoliths are the most ancient, abundant and continuous record of pelagic photic zone calcite producer organisms. Hence, they could be valuable substrates for geochemically based paleoenvironmental reconstructions but only Sr/Ca is exploited even if ~~it remained partially understood~~. For example, some murolith coccoliths species have very high Sr/Ca compared to the common 1-4 mmol/mol recorded in placolith coccoliths. In this study, we analyzed the elemental composition of the Middle Jurassic murolith *Crepidolithus crassus* by synchrotron-based nanoXRF (X-ray Fluorescence Spectroscopy) mapping focusing on Sr/Ca and compared the record to two placolith species, namely *Watznaueria contracta* and *Discorhabdus striatus*. In *C. crassus*, Sr/Ca is more than ten times higher than in both placoliths and seems higher in the proximal cycle. By comparison with the placoliths analyzed in the same analytical set-up and from the same sample, we exclude the impact of the diagenesis and seawater Sr/Ca to explain the high Sr/Ca in *C. crassus*. Based on comparisons to *Pontosphaera discopora* and *Scyphosphaera apsteinii* which also have high Sr/Ca, it seems more likely that high Sr/Ca in *C. crassus* is either due to the vertical elongation of the R-units of the proximal cycle or related to the action of the special polysaccharide controlling the growth of those vertically elongated R-units that may have affinities to Sr^{2+}. In order to apply the Sr/Ca proxy to muroliths, further investigations are needed on ~~culture experiments~~.

1. Introduction

Paleoceanography partly relies on the application of geochemical proxies – *i.e.* chemical changes of fossils or sediments composition induced by chemical, physical or biological parameters changing through time. Many geochemical proxies are based on elemental ratios in planktic or benthic foraminifera *e.g.* Mg/Ca (temperature; Elderfield and Ganssen, 2000), B/Ca (pH, Yu et al., 2007), U/Ca (carbonate saturation, Raitzsch et al., 2011), Cd/Ca (paleonutrient, Rickaby and Elderfield, 1999). Conversely, calcareous nannofossils – the micrometric platelets called coccoliths produced by the photosynthetic unicellular algae called coccolithophore and other micrometric calcite *incertae sedis* – are rarely used for geochemistry in palaeoceanography. The rarity of nannofossil-based geochemical palaeoproxies is linked to the very small size of calcareous nannofossils – *i.e.* ~1-15 µm – increasing the difficulty to isolate them from the rest of the sediment (Stoll and Ziveri, 2002; Stoll and Shimizu, 2009; Minoletti et al., 2009; Suchéras-Marx et al., 2016a). The only proxy commonly based on the calcareous nannofossil chemical composition is the Sr/Ca ratio used as a palaeoproductivity proxy (Stoll and Schrag, 2000).

The Sr/Ca ratio in calcareous nannofossils is a relative proxy which has no quantitative calibration. The process underlying the positive relation between Sr/Ca and productivity stands on the observation that more Sr is incorporated in calcite with high calcification rates which positively correlates with high cell physiological rates. This proxy is also species-dependent or, at least, *group*-dependent (Stoll and Ziveri, 2004). The latter is discussed, the species-dependency may be related to different calcification physiologies (Payne et al., 2008; Suchéras-Marx et al., 2016b) or to different partitioning coefficients in relation to different ultrastructure organizations and more precisely between V- and R- crystals in coccoliths (Young et al., 1992) theoretically possible (Paquette and Reeder, 1995) but still not observed (Stoll and Ziveri, 2004).

Recently, analyses on the cultured murolith *Scyphosphaera apsteinii* showed Sr/Ca ~22 mmol/mol, an order of magnitude higher than the common ~1-4 mmol/mol measured in placoliths such as *Gephyrocapsa oceanica*, *Gephyrocapsa huxleyi*, *Calcidiscus leptoporus*, *Coccolithus pelagicus* or *Helicosphaera carteri* (Hermoso et al., 2017; Stoll et al., 2007). Hermoso et al. (2017) also highlight observations of high Sr/Ca in fossil muroliths *Pontosphaera* (Pliocene) and *Crepidolithus* (Lower Jurassic) but points out that *Scyphosphaera*, *Pontosphaera* and *Crepidolithus* have different crystal organizations and growth directions and thus crystal organization cannot explain murolith high Sr/Ca.

The present study aims to map Sr and Ca in *Crepidolithus crassus* and to compare the calculated Sr/Ca with the crystal growth directions in order to explain the murolith Sr anomaly. Analyses are based on synchrotron XRF with high-spatial resolution using the set-up of ESRF beamline ID22 (now

ID16B) and compared to placoliths. The two placolith species are from the same sample considered as control species for paleoenvironmental conditions and diagenesis overprint.

2. Materiel and methods

2.1. Sample preparation

The coccolith analyzed in this study comes from sample CM35, a marlstone from the Lower Bajocian (Middle Jurassic) of Cabo Mondego (Portugal; section in Suchéras-Marx et al., 2012). A total of three coccoliths from three different species were studied, namely the murolith *Crepidolithus crassus* and two placoliths *Discorhabdus striatus* and *Watznaueria contracta*. The three coccoliths were picked using Suchéras-Marx et al. (2016a) protocol and mounted on 500 nm-thick silicon nitride (Si_3N_4) TEM windows (Silson Ltd. Southam, UK).

2.2. NanoXRF 17 keV mapping at ID22NI

All three coccoliths were analyzed at an incident X-ray beam energy of 17 keV at ID22NI (currently ID16b), 100 nm x 100 nm beam spot size focused by an ESRF custom-made Kirkpatrick-Baez double multilayer mirror device and 2 s dwell time per pixel. The detectors were high-count rate twin SII™ vortex SDD (silicon drift diode) detectors, capable of counting up to 200 kcps with no saturation and no peak shift or FWHM broadening, when operated below 10% dead time. The maps were made with adjacent spots of analysis. The beam line set-up, analysis procedure and calculation fit are the same as in Suchéras-Marx et al. (2016b).

3. Results

3.1. XRF spectrum

The three spectra shown in Fig. 1 represent the mean spectrum for each coccolith. Because XRF analysis is penetrative, the spectra also record the membrane holding the coccolith and thus the spectrum of zones with only the membrane is also presented. The fit presented for each spectrum is the modeled reconstruction used for the calculation and the map reconstruction (cps and mmol/mol). In *D. striatus* and *W. contracta*, 14 elements are recorded namely: S, Cl, Ar, K, Ca, Mn, Fe, Cu, Zn, Br, Kr, Rb, Sr and Pb whereas in *C. crassus* only 12 are recorded (same elements except Kr and Rb) (Fig. 1). The rare gases Ar and Kr are present in the air in the experimental hutch. The contribution of the membrane is lower than 1% for Ca and Sr and thus is negligible for the Sr/Ca calculation. Nevertheless, membrane contribution was excluded in Table 1. Those results are similar to already published *W. britannica* and *D. striatus* (Suchéras-Marx et al., 2016b; Suchéras-Marx et al., 'submitted').

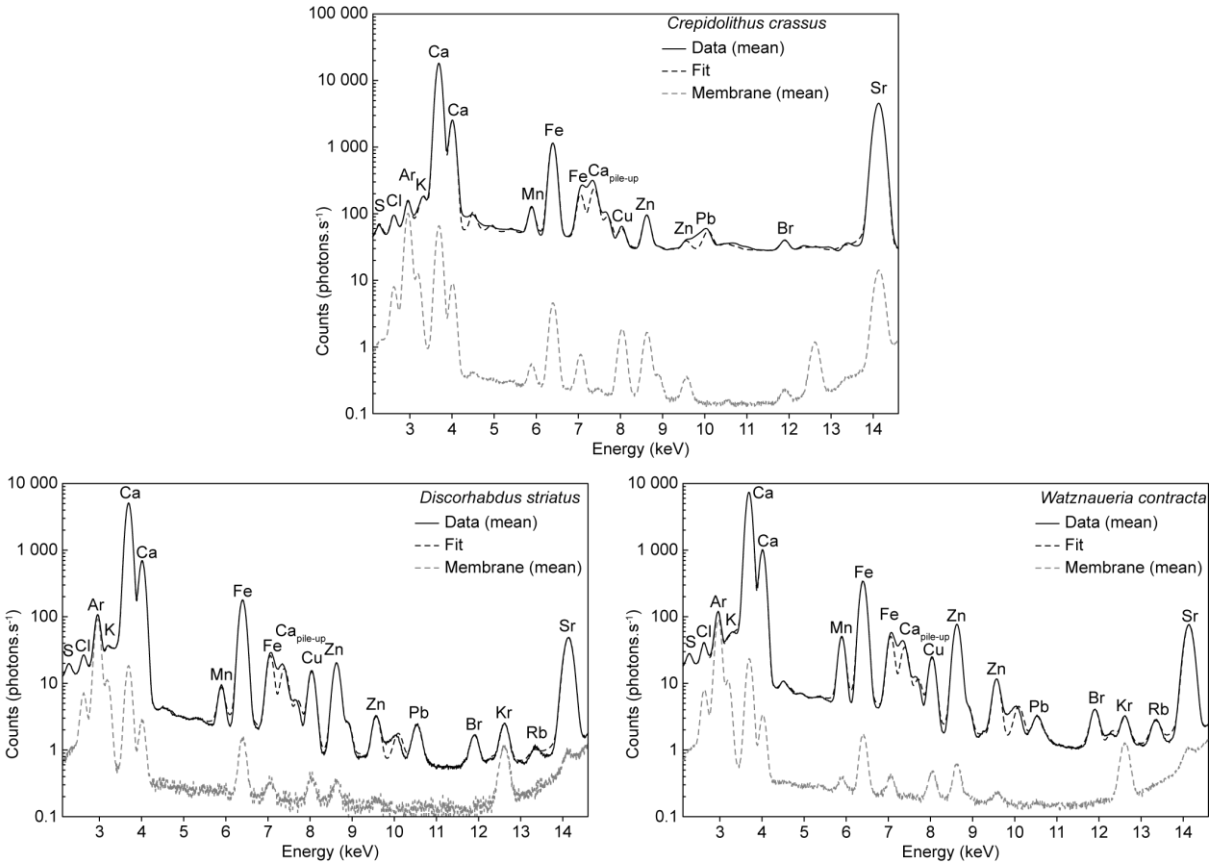

Figure 1: Mean XRF spectra of *C. crassus*, *D. striatus* and *W. contracta* coccoliths and associated membrane spectra.

3.2. Element and ratio maps

For the three coccoliths, element maps of Ca, Mn and Sr are presented in Fig. 2 (cps) and the three maps together in color in Supplementary Figure 1. Direct comparison of Ca and Sr is possible in both placoliths whereas Mn is quite different although crystal organization is also observed in this element map. In *W. contracta*, the Ca maps are precise enough to recognize the shield crystal orientations, especially the outer radial growth from the tube ring. The tube structures are difficult to recognize but still, crystals can be seen in the rim around the central area. In the Sr map of the same species, the outer rim with radial crystals of the shields are easily observed too. A ring with slightly more Sr marks a boundary between the outer rim and the inner rim structures. These inner rim structures are composed of two concentric rings of crystal assemblages. The outermost one may correspond to the mid tube elements whereas the innermost one may correspond to the inner tube elements. The mid tube elements form a clear rim whereas one shield crystal assemblage is nicely depicted in the Mn map (Suchéras-Marx et al., 2016b). In *D. striatus*, the Sr seems less abundant in the tube units in comparison to the shield elements. For the same species, the Mn is scarce in the central area and the tube structures but more abundant in the shields.

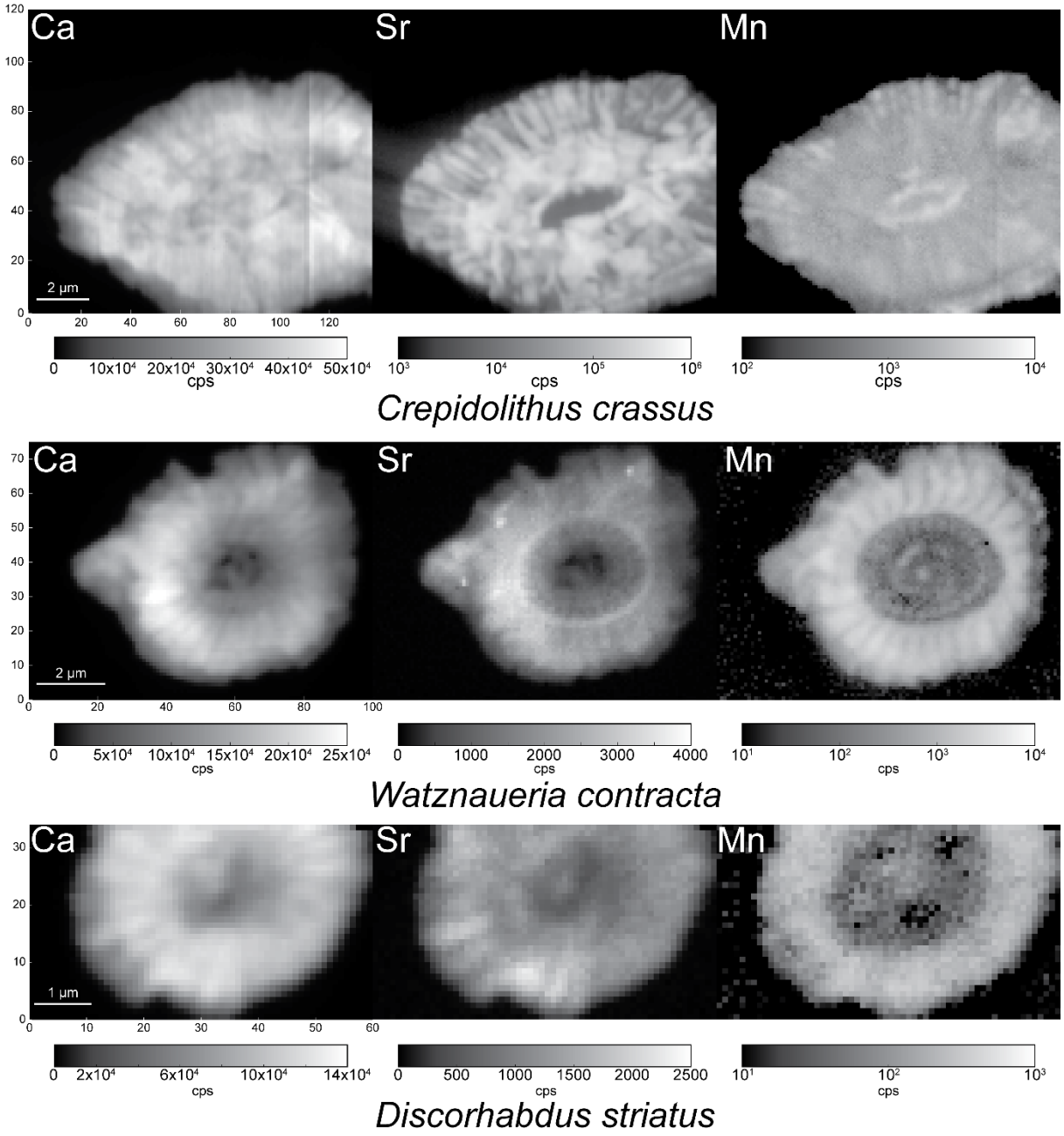

Figure 2: Ca, Mn and Sr maps (cps) of *C. crassus*, *D. striatus* and *W. contracta*.

Conversely to the placoliths, in *C. crassus*, the Ca and Sr maps are slightly different. In Sr maps, the central area is easily visible. Around the central area, an inner concentric rim of more abundant Sr is observed. A concentric outer rim up to the lateral border is observed with Sr concentrated in radial rays. In the Ca map, the outer rim is also observed in radial structures but the inner rim is distinguished from the outer only by a discontinuity. Finally, another discontinuity separates the central area from the inner rim.

	Mean whole coccolith		Selected zone	
element ratio (mmol/mol)	Mn/Ca	Sr/Ca	Mn/Ca	Sr/Ca
Crepidolithus crassus	0.75	9.82	0.70	11.57
Discorhabdus striatus	0.23	0.38	0.12	0.33
Watznaueria contracta	1.10	0.40	0.36	0.43

Table 1: Mn/Ca and Sr/Ca (mmol/mol) of whole coccoliths of *C. crassus*, *D. striatus* and *W. contracta* or a selected region, depleted in Mn and Fe.

For all species, the Sr/Ca maps have the same patterns as Sr and similarly, the Mn/Ca maps have the same patterns as Mn (Fig. 3). In *C. crassus* then, the Sr/Ca is higher in a ring around the central area and in radially oriented crystals in the outer ring. In the most concentrated area, the Sr/Ca ranges between 10 and 100 mmol/mol and tends to be two orders of magnitude higher than in *W. contracta* and *D. striatus*. Finally, the area with higher Sr/Ca is neither enriched nor depleted in Mn/Ca.

4. Discussion

A previous study already discussed the Sr/Ca signal in *Watznaueria* (Suchéras-Marx et al., 2016b), discussion that likely applies to *Discorhabdus*. Another study discussed the use of Mn as an overgrowth and diagenesis tracer in both *Watznaueria* and *Discorhabdus* (Suchéras-Marx et al., submitted). Therefore, the placolith signal won't be discussed here. The three coccoliths are coming from the same sample and were analyzed with the same set-up, thus the very high Sr/Ca in *C. crassus* compared to *W. contracta* and *D. striatus* is not related to analytical biases and to seawater Sr/Ca. Moreover, the Sr-rich rim in *C. crassus* is not enriched in Mn and thus the high Sr/Ca in *C. crassus* is not related to diagenesis. This result is coherent with a previous study observing that diagenesis tends to lower Sr/Ca in calcareous nannofossils (Dedert et al., 2014).

The Sr anomaly in *C. crassus* is then related to either i) an ion pump concentrating the Sr^{2+} inside the cell to higher concentrations than other species; ii) the use of a polysaccharide that tends to increase Sr/Ca in comparison to other species or iii) the crystal organization and growth directions which are controlled by the cell but the high concentration in Sr would then be a by-product of the coccolith construction. Obviously, *C. crassus* being a fossil occurring only during the Jurassic, the cell biology of the species cannot be explored. Nevertheless, this species is a large murolith like the extant *Pontosphaera discopora* and has a similar shape to the extant *Scyphosphaera apsteinii*'s lopadolith, both having also higher Sr/Ca than the common placoliths' signature of 1-4 mmol/mol (Hermoso et al., 2017).

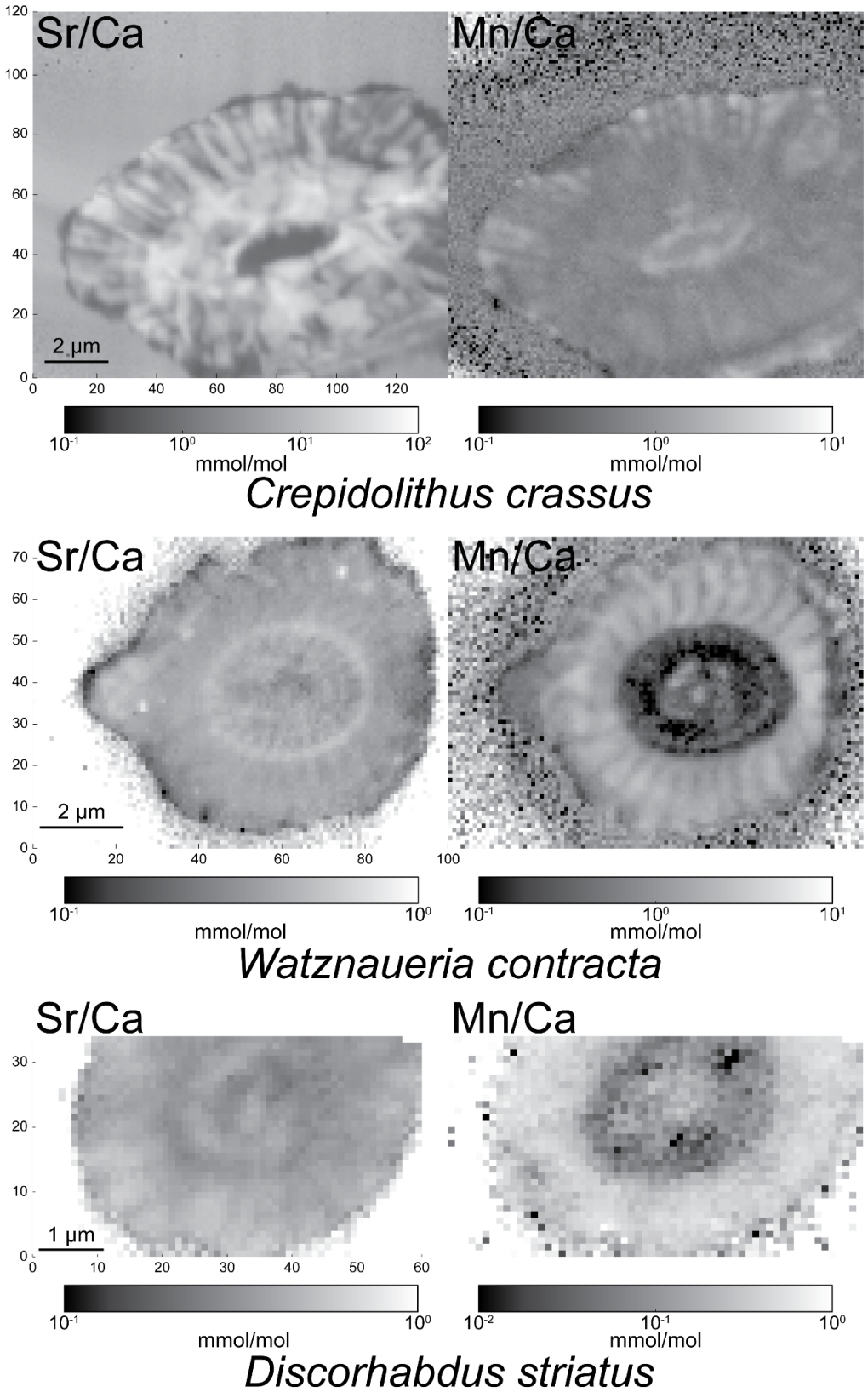

Figure 3: Mn/Ca and Sr/Ca (mmol/mol) maps of *C. crassus*, *D. striatus* and *W. contracta*.

The first two hypotheses could be inherited in descendant species from *C. crassus*. Both *Pontosphaera* and *Scyphosphaera* are very closely related in the coccolithophore phylogeny (Family

Pontosphaeraceae; de Vargas et al., 2007). *Crepidolithus* is within the Family Chiastozygaceae (Bown and Young, 1998), whose position is unknown, but could be the Family ancestor of the Family Zygodiscaceae and its descendants, the Families Pontosphaeraceae and Helicosphaeraceae (Bown and Young, 1998). Thus, the high Sr/Ca in both *Pontosphaera* and *Scyphosphaera* could be an ancestral character inherited from *Crepidolithus*. This hypothesis may be challenged by *Helicosphaera carterii* which has a Sr/Ca ratio around 2-3 mmol/mol (Stoll and Ziveri, 2004) and is from the Family Helicosphaeraceae, the sister group of the Family Pontosphaeraceae. The low Sr/Ca in *H. carterii* could then be a derived character in the phylogeny, arguing for a phyletic heritage of *Pontosphaera* and *Scyphosphaera* from *Crepidolithus* or this character is ancestral in the Family Helicosphaeraceae and the Sr/Ca is not linked to the phylogeny. The current phyletic and Sr/Ca data cannot exclude one or the other solutions, hence a possible ion pump or polysaccharide could have favored the high Sr/Ca in *C. crassus*.

The last hypothesis relies ~~in~~ the fact that *C. crassus*, *P. discopora* and *S. apsteinii* have the same shape (*i.e.* murolith and lopadolith) and are very large coccoliths, thus the shape and size may influence the Sr incorporation in coccolith calcite. The large size of those coccoliths cannot be the main reason of high Sr/Ca because *Coccolithus braarudii*, a very large placolith, has Sr/Ca equivalent to very small placoliths (*i.e. G. huxleyi*; Müller et al., 2011). The basic crystal organization of heterococcoliths is explained by the V/R model which describes the crystal growth in the *c-axis* whether radially (*i.e.* R-unit) or vertically (*i.e.* V-unit) from a primary ring of crystals called protococcolith (Young et al., 1992). In *C. crassus*, the V-units are more developed than the R-units (Fig. 4), whereas in *P. discopora* and *S. apsteinii* V-units represent only the narrow outer part of the rim wall (Young and Bown, 1997; Fig. 4). According to Hermoso et al. (2017), the growth of calcite in the same direction as the *c-axis* should favor Sr^{2+} incorporation but the R-units in *P. discopora* and *S. apsteinii* actually grow longer in the vertical axis hence grow orthogonally to the *c-axis*. In the case of *C. crassus*, the Sr/Ca is higher around the central area which corresponds to the proximal cycle formed by R-units. Counter-intuitively for these three species with thick vertical walls, the Sr is concentrated in the R-units. Surprisingly, *C. crassus* R-units are, like *P. discopora* and *S. apsteinii*, more elongated vertically than radially, thus the growth seems orthogonal to the *c-axis* (Fig. 4). Then, either the orthogonal to *c-axis* growth actually favors Sr^{2+} contradicting Hermoso et al. (2017) or the biomolecule acting in this growth direction has more affinities with Sr^{2+} than the other polysaccharides.

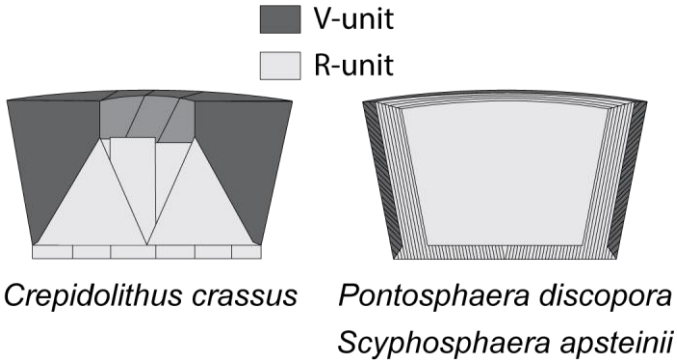

Figure 4: Crystal assembly of *Crepidolithus*, *Pontosphaera* and *Scyphosphaera*. R-units (light grey) and V-units (dark grey), derived from Bown and Young, 1998.

5. Conclusion

Despite the very high and continuous fossil record of coccoliths since the Late Triassic, the geochemical analyses of these platelets for paleoenvironmental reconstructions remain rare. So far, coccolith Sr/Ca is the only coccolith-based geochemical proxy commonly used in paleoceanography. Yet, there are many unknown features about this productivity proxy such as the very high Sr/Ca in some species namely *S. apsteinii*, *P. discopora* and *C. crassus*. In this study, we compared Sr/Ca of *C. crassus* to contemporaneous placoliths using synchrotron-based nanoXRF and observed that:

- *C. crassus* has higher Sr/Ca than contemporaneous placoliths;
- *C. crassus* Sr/Ca map is different than the Mn/Ca map
- Sr/Ca in *C. crassus* is higher in the proximal cycle than in the distal cycle

Hence, high *C. crassus* Sr/Ca, is not linked to diagenetic overgrowth or seawater Sr/Ca but may be related to vertical elongation of R-units and/or affinity to Sr^{2+} of the polysaccharide responsible for the growth of those peculiar R-units. The use of murolith's Sr/Ca in the future may be interesting due to their high values, easier to measure and to the large size of these coccoliths, easier to separate from the bulk placoliths. Nevertheless, in order to apply the Sr/Ca productivity proxy to muroliths in the future, new culture studies should test the relation between Sr incorporation and growth rate and clearly identify the origin of the Sr anomaly in those coccoliths.

Author contributions

BSM, FG and ID designed the study with later contribution from AS. BSM, FG, ID, AS and RT did the analyses. BSM performed the data treatment with help from AS. BSM wrote the manuscript with comments from all contributors.

Acknowledgments

We acknowledge the ESRF for providing access to synchrotron radiation on the ID22NI beamline through proposal EC811. This study is a contribution to the Cerege's team 'Climat'.

Data accessibility

Data presented in this study are freely accessible on PANGAEA database (https://doi.org/10.1594/PANGAEA.913826). Related data produced with similar material and during the same ESRF experiment (project EC811) are also accessible on PANGAEA with https://doi.pangaea.de/10.1594/PANGAEA.913813 published in Suchéras-Marx et al. (2016), https://doi.pangaea.de/10.1594/PANGAEA.913811 in Suchéras-Marx et al. (submitted) and unpublished data (https://doi.pangaea.de/10.1594/PANGAEA.914203).

References

Bown, P.R., Young, J.R., 1998. Introduction in: Bown, P.R. (Ed.), Calcareous nannofossil biostratigraphy. British Micropaleontological Society Publication Series. Chapman and Hall (Kluwer Academic Publishers), Dondrecht, pp. 1-15

Dedert, M., Stoll, H.M., Kars, S., Young, J.R., Shimizu, N., Kroon, D., Lourens, L.J., Ziveri, P., 2014. Temporally variable diagenetic overgrowth on deep-sea nannofossil carbonates across Palaeogene hyperthermals and implications for isotopic analyses. Marine Micropaleontology 107, 18-31.

Elderfield, H., Ganssen, G., 2000. Past temperature and $\delta^{18}O$ of surface ocean waters inferred from foraminiferal Mg/Ca ratios. Nature 405, 442-445.

Hermoso, M., Lefeuvre, B., Minoletti, F., de Rafélis, M., 2017. Extreme strontium concentrations reveal specific biomineralization pathways in certain coccolithophores with implications for the Sr/Ca paleoproductivity proxy. PLOS ONE 12, e0185655.

Minoletti, F., Hermoso, M., Gressier, V., 2009. Separation of sedimentary micron-sized particles for palaeoceanography and calcareous nannoplankton biogeochemistry. Nature Protocols 4, 14-24.

Müller, M.N., Kisakürek, B., Buhl, D., Gutperlet, R., Kolevica, A., Riebesell, U., Stoll, H., Eisenhauer, A., 2011. Response of the coccolithophores *Emiliania huxleyi* and *Coccolithus braarudii* to changing seawater Mg^{2+} and Ca^{2+} concentrations: Mg/Ca, Sr/Ca ratios and $\delta^{44/40}Ca$, $\delta^{26/24}Mg$ of coccolith calcite. Geochimica et Cosmochimica Acta 75, 2088-2102.

Paquette, J., Reeder, R.J., 1995. Relationship between surface structure, growth mechanism, and trace element incorporation in calcite. Geochimica et Cosmochimica Acta 59, 735-749.

Payne, V.E., Rickaby, R.E.M., Benning, L.G., Shaw, S., 2008. Calcite crystal growth orientation: implications for trace metal uptake into coccoliths. Mineralogical Magazine 72, 269-272.

Raitzsch, M., Kuhnert, H., Hathorne, E.C., Groeneveld, J., Bickert, T., 2011. U/Ca in benthic foraminifers: A proxy for the deep-sea carbonate saturation. Geochemistry, Geophysics, Geosystems 12, Q06019.

Rickaby, R.E.M., Elderfield, H., 1999. Planktonic foraminiferal Cd/Ca: Paleonutrients or Paleotemperature? Paleoceanography 14, 293-303.

Suchéras-Marx, B., Guihou, A., Giraud, F., Lécuyer, C., Allemand, P., Pittet, B., Mattioli, E., 2012. Impact of the Middle Jurassic diversification of *Watznaueria* (coccolith-bearing algae) on the carbon cycle and $\delta^{13}C$ of bulk marine carbonates. Global and Planetary Change 86-87, 92-100.

Suchéras-Marx, B., Giraud, F., Lena, A., Simionovici, A., 2016a. Picking nannofossils: How and why. Journal of Micropalaeontology 36, 219-221.

Suchéras-Marx, B., Giraud, F., Simionovici, A., Daniel, I., Tucoulou, R., 2016b. Perspectives on heterococcolith geochemical proxies based on high-resolution X-ray fluorescence mapping. Geobiology 14, 390-403.

Suchéras-Marx, B., Giraud, F., Daniel, I., Rivard, C., Aubry, M.-P., Baumann, K.-H., Beaufort, L., Tucoulou, R., Simionovici, A., Submitted. Origin of manganese in coccolith calcite based on synchrotron nanoXRF and XANES. Marine Micropaleontology.

*Preprint version: Suchéras-Marx, B., Giraud, F., Daniel, I., Rivard, C., Aubry, M.P., Baumann, K.-H., Beaufort, L., Tucoulou, R., Simionovici, A., 2020. Origin of manganese in nannofossil calcite based on synchrotron nanoXRF and XANES, PaleorXiv. 10.31233/osf.io/p8cn5

Stoll, H.M., Schrag, D.P., 2000. Coccolith Sr/Ca as a new indicator of coccolithophorid calcification and growth rate. Geochemistry, Geophysics, Geosystems 1, 1006.

Stoll, H.M., Shimizu, N., 2009. Micropicking of nannofossils in preparation for analysis by secondary ion mass spectrometry. Nature Protocols 4, 1038-1043.

Stoll, H.M., Ziveri, P., 2002. Separation of monospecific and restricted coccolith assemblages from sediments using differential settling velocity. Marine Micropaleontology 46, 209-221.

Stoll, H.M., Ziveri, P., 2004. Coccolithophorid-based geochemical paleoproxies, in: Thierstein, H.R., Young, J.R. (Eds.), Coccolithophores: From molecular processes to global impact. Springer, Verlag, pp. 529-562.

Stoll, H.M., Shimizu, N., Arevalos, A., Matell, N., Banasiak, A., Zeren, S., 2007. Insights on coccolith chemistry from a new ion probe method for analysis of individually picked coccoliths. Geochemistry, Geophysics, Geosystems 8, Q06020.

Vargas, C. de, Aubry, M.-P., Probert, I., Young, J.R., 2007. Origin and evolution of coccolithophores: From coastal hunters to oceanic farmers, in: Falkowski, P.G., Knoll, A. (Eds.), Evolution of primary producers in the sea. Academic Press, pp. 251-286.

Young, J.R., Bown, P.R., 1997. Higher classification of calcareous nannofossils. Journal of Nannoplankton Research 19, 15-20.

Young, J.R., Didymus, J.M., Bown, P.R., Mann, S., 1992. Crystal assembly and phylogenetic evolution in heterococcoliths. Nature 356, 516-518.

Yu, J., Elderfield, H., Hönish, B., 2007. B/Ca in planktonic foraminifera as a proxy for surface seawater pH. Paleoceanography 22, 2202.

Supplementary figure

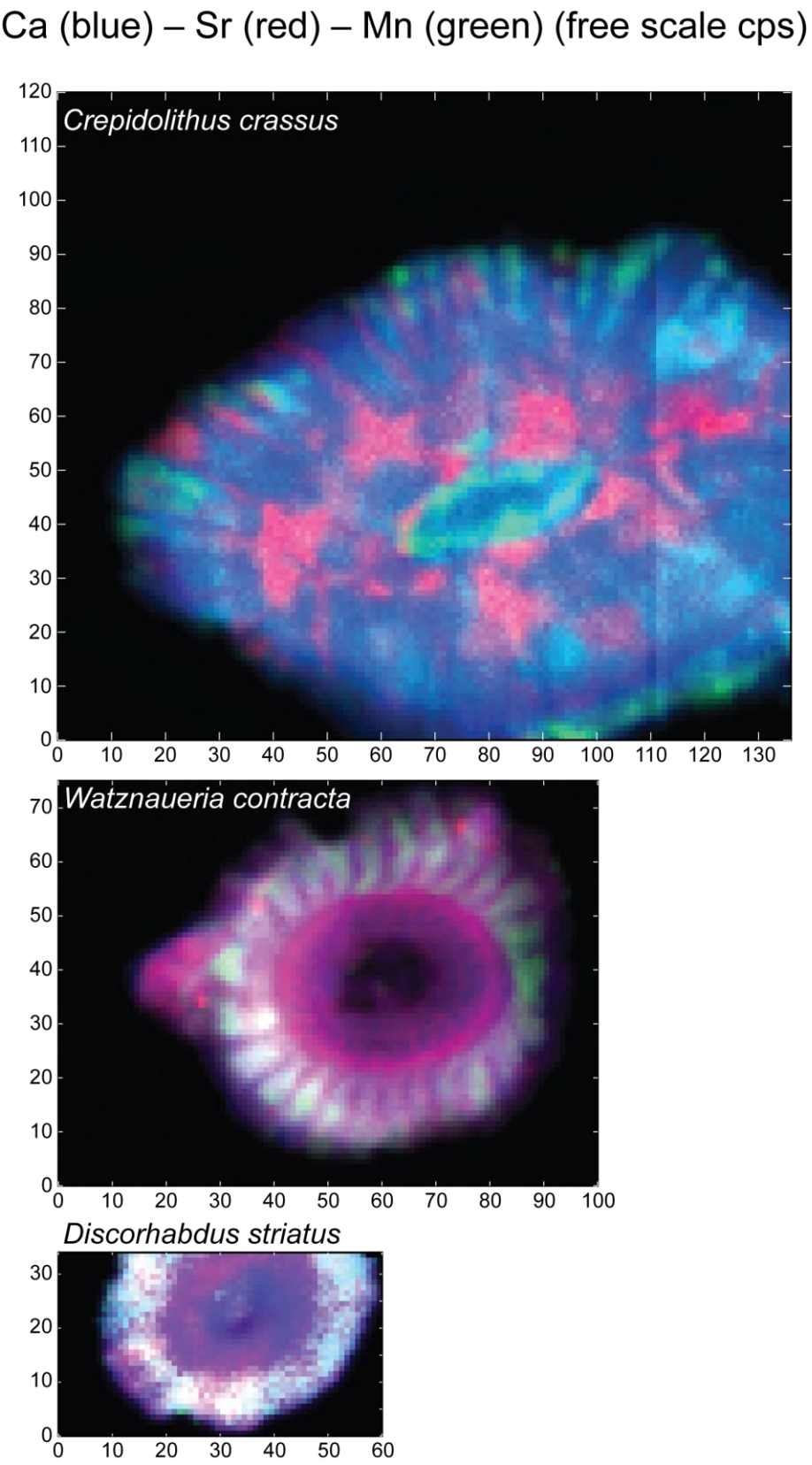

Supplementary Figure 1: Ca (blue), Sr (red) and Mn (green) maps (free scale cps) of *C. crassus*, *W. contracta* and *D. striatus*.